Cerebral Cortex November 2012;22:2634–2642
doi:10.1093/cercor/bhr350
Advance Access publication December 9, 2011

KCTD8 Gene and Brain Growth in Adverse Intrauterine Environment: A Genome-wide Association Study

Tomáš Paus[1,2], Manon Bernard[3], M. Mallar Chakravarty[1], George Davey Smith[4], Jesse Gillis[5], Anbarasu Lourdusamy[6], Melkaye G. Melka[3], Gabriel Leonard[2], Paul Pavlidis[5], Michel Perron[7], G. Bruce Pike[2], Louis Richer[7], Gunter Schumann[6], Nicholas Timpson[4], Roberto Toro[8], Suzanne Veillette[9] and Zdenka Pausova[3]

[1]Rotman Research Institute, University of Toronto, Toronto, Ontario M6A 2E1, Canada, [2]Montreal Neurological Institute, McGill University, Montreal, Quebec H3A 2B4, Canada, [3]Hospital for Sick Children, University of Toronto, Toronto, Ontario M5G 1X8, Canada, [4]Department of Social Medicine, University of Bristol, Bristol BS8 2BN, UK, [5]Centre for High-Throughput Biology and Department of Psychiatry, University of British Columbia, Vancouver V6T 1Z4, Canada, [6]Medical Research Council–Social, Genetic and Developmental Psychiatry Centre, Institute of Psychiatry, King's College, London SE5 8AF, UK, [7]Department of Health Sciences, University of Quebec in Chicoutimi, Chicoutimi, Quebec G7H 2B1, Canada, [8]Institut Pasteur, Paris 75724, France and [9]CEGEP Jonquière, Jonquière, Quebec G7X 3W1, Canada

Address correspondence to Tomas Paus. Email: tpaus@rotman-baycrest.on.ca.

The most dramatic growth of the human brain occurs in utero and during the first 2 years of postnatal life. Genesis of the cerebral cortex involves cell proliferation, migration, and apoptosis, all of which may be influenced by prenatal environment. Here, we show that variation in *KCTD8* (potassium channel tetramerization domain 8) is associated with brain size in female adolescents (rs716890, $P = 5.40 \times 10^{-09}$). Furthermore, we found that the *KCTD8* locus interacts with prenatal exposure to maternal cigarette smoking vis-à-vis cortical area and cortical folding: In exposed girls only, the *KCTD8* locus explains up to 21% of variance. Using head circumference as a proxy of brain size at 7 years of age, we have replicated this gene–environment interaction in an independent sample. We speculate that *KCTD8* might modulate adverse effects of smoking during pregnancy on brain development via apoptosis triggered by low intracellular levels of potassium, possibly reducing the number of progenitor cells.

Keywords: adolescence, brain, GWAS, pregnancy

Introduction

In humans, the genesis of the cerebral cortex begins during the first trimester (~6 weeks of gestation) and, in this early developmental phase, involves symmetrical divisions of neuroepithelial progenitor cells in the ventricular zone. Around week 12 of gestation, neurogenesis commences with a gradual switch toward asymmetric divisions of the progenitor cells and migration of postmitotic neurons away from the ventricular zone (reviewed in Chan et al. 2002). During the second and third trimester of gestation, the human brain grows exponentially, reaching ~420 cm^3 in volume (~36% of adult values) at birth (Knickmeyer et al. 2008). Postnatal growth is particularly rapid during the first 2 years: the brain volume doubles by the end of the first year (855 cm^3; 72% of adult) and increases further to reach 83% (983 cm^3) of adult values by the end of the second year (Knickmeyer et al. 2008). In the cerebral hemispheres, most of this growth takes place in the cortical gray matter (Knickmeyer et al. 2008).

Gross disturbances in brain development result in microcephaly and/or lissencephaly, the former typically defined as a head circumference (HC) smaller than 2 standard deviations (SDs) below the mean (Opitz and Holt 1990). Several genes have been associated with these developmental abnormalities, including *MCPH1* through *MCPH7*, *LIS1*, and *DCX*; most of these genes are involved in regulating some aspects of self-renewal (i.e., symmetric division) of the progenitor cells (reviewed in Mochida 2009).

Cell proliferation and programmed cell death (apoptosis) are the key processes that, in combination, determine the final number of neurons constituting, together with glial cells, the cerebral cortex. Apoptosis can affect progenitor cells and thus influence the overall number of postmitotic neurons migrating away from the ventricular zone, or it could regulate the number of surviving neurons once they reached the cerebral cortex (Kuan et al. 2000). Apoptotic nuclei have been detected in the human brain both in the ventricular zone (~5 week of gestation; Rakic and Zecevic 2000) and in the developing telencephalon (~12 to 22 weeks; Chan and Yew 1998; Rakic and Zecevic 2000). Proapoptotic (e.g., *Bax* and *Bcl-X_S*) and antiapoptotic (e.g., *Bcl-X_L*) genes of the *Bcl2* family interact and, together with other proapoptotic genes (*caspase 3*, *caspase 9*, and *Apaf1*), regulate apoptosis during brain development in both global- and region-specific manner (Kuan et al. 2000). The rates of cell proliferation and apoptosis during prenatal and early postnatal development, together with the corresponding growth of neuropil and white matter, determine brain size. Interindividual variations in brain volume and total cortical area are considerable. For example, brain volumes calculated from magnetic resonance images (MRI) obtained in healthy individuals vary approximately between 1140 and 1550 cm^3 in males and 1020 and 1380 cm^3 in females (these values were estimated from the mean ± 2 SDs of brain volume in samples of 1231 males and 1109 females reviewed in Paus 2010a). Despite the high heritability (~80%) of brain volume assessed in twin cohorts (e.g., Giedd et al. 2007), only a single study reported gene loci associated with this phenotype in healthy individuals, as revealed by a genome-wide search (Seshadri et al. 2007).

Given the critical importance of developmental processes taking place in utero, deprivation of the fetus of various macro- and micronutrients and oxygen, as well as its exposure to toxins, such as alcohol, are likely to have a significant and long-lasting impact on the brain, especially when acting together (Guerrini et al. 2007). Maternal smoking of cigarettes during pregnancy generates an adverse intrauterine environment impacting the developing fetus in several ways: 1) inhaled nicotine induces vasoconstriction of the uteroplacental vasculature, leading to uteroplacental underperfusion and, in turn, decreased flow of nutrients and oxygen to the fetus; 2) increased levels of carboxyhemoglobin reduce tissue oxygenation of the fetus;

3) nicotine suppresses the mother's appetite, leading to reduced energy intake by the mother and, hence, reduced energy supply to the fetus; and 4) nicotine causes alterations in the cellular growth and activity of the central and peripheral nervous system (Lambers and Clark 1996; Slotkin 1998). In our previous work, we have described associations between cigarette smoking during pregnancy and the size of the corpus callosum (Paus et al. 2008) as well as cortical thickness (Toro et al. 2008) in the adolescent offspring. Here, we employ this particular form of early adversity to examine its possible modulating effect on the genotype–phenotype relationship revealed in a genome-wide association study (GWAS) of the brain volume and associated cortical phenotypes.

We report findings obtained in vivo with MRI in typically developing adolescents participating in the Saguenay Youth Study (Pausova et al. 2007). This study takes place in a region with a known genetic founder effect (De Braekeleer 1991, 1998; Grompe et al. 1994); all participants are of single ethnicity (White Caucasians of French descent). The study was designed to evaluate possible adverse effects of maternal smoking during pregnancy; half of the participants were exposed to maternal smoking during pregnancy, and the other (nonexposed) half were matched to the exposed by maternal education and school attended in order to minimize group differences in various socioeconomic indicators. First, we carried out a GWAS to identify gene loci associated with the total brain volume. Next, we tested the main effect of the *KTCD8* locus, revealed as significant at a genome-wide level in girls, and its interaction with prenatal exposure to maternal cigarette smoking (PEMCS) on cortical area and cortical folding. We have also evaluated these factors vis-à-vis indicators of an overall prenatal (birth weight) and postnatal (height) growth. Finally, we used HC measured at birth and at 7 years of age as a proxy of brain size and replicated the interaction between genetic variations in the *KCTD8* locus and PEMCS in an independent sample.

Materials and Methods

Discovery Sample: The Saguenay Youth Study

Participants

Adolescent siblings and their biological parents were recruited from a population with a known founder effect, namely Saguenay–Lac-Saint-Jean region of Quebec, Canada. Both maternal and paternal grandparents of the adolescents were of French–Canadian ancestry born in the region; as such, all adolescents are of a single ethnicity, namely white Caucasians of French–Canadian ancestry. The current data set consisted of 599 12- to 18-year-old adolescents; following quality control of the brain phenotypes and genotypes, 557 adolescents (267 males, 180 ± 22 months of age [Mean ± SD]; 290 females, 182 ± 23 months of age) were included in the final analyses.

Adolescents were recruited as previously reported (Pausova et al. 2007). Briefly, recruitment begins with the team visiting all classrooms in a given secondary school and presenting the study to the students. Concurrently, an information brochure, a letter from the principal, and a consent form for a telephone interview are mailed to the parents. Subsequently, a research nurse conducts a telephone interview with interested families, usually with the child's biological mother, to verify their eligibility. Additional information is acquired using a medical questionnaire completed by the child's biological parent.

The main exclusion criteria for both exposed and nonexposed adolescents are 1) positive medical history for meningitis, malignancy, and heart disease requiring heart surgery; 2) severe mental illness (e.g., autism, schizophrenia) or mental retardation (IQ < 70); 3) premature birth (<35 weeks); and 4) MRI contraindications. The following inclusion criteria are used for both exposed and nonexposed adolescents: 1) age 12–18 years; 2) one or more siblings in the same age group; and 3) maternal and paternal grandparents of French–Canadian ancestry. Exposed adolescents must have positive history of maternal cigarette smoking (>1 cigarette/day in the second trimester of pregnancy). The nonexposed adolescents are matched to the exposed ones based on the level of maternal education and the school attended. In the case of mothers of nonexposed offspring, we require negative history of maternal cigarette smoking during pregnancy and during the 12-month period preceding the pregnancy. For both the mothers of exposed and nonexposed adolescents, we require negative history of excessive alcohol use during pregnancy (>210 mL/week). Cigarette smoking before and during pregnancy is ascertained retrospectively by a research nurse during a structured telephone interview with the mother. We assessed the overall agreement between the exposure status noted in the medical records at the time of pregnancy and by the maternal report during the telephone interview using a Kappa statistics and found a value of 0.69 ± 0.04 indicating a "good" agreement (Pausova et al. 2007). A number of health behaviors associated with smoking during pregnancy and early postnatal period have been acquired through self-reports by the mothers, together with information about pregnancy and birth as well as socioeconomic descriptors of the family (see Table 1).

The Research Ethics Committee of the Chicoutimi Hospital approved the study protocol.

Magnetic Resonance Imaging: Acquisition and Analysis

MR images were acquired on a Phillips 1.0-T superconducting magnet. High-resolution anatomical T_1-weighted (T1W) images were acquired using the following parameters: 3D radio frequency-spoiled gradient echo scan with 140–160 sagittal slices, 1-mm isotropic resolution, time repetition = 25 ms, time echo = 5 ms, and flip angle = 30°. We measured cortical thickness using FreeSurfer, a set of automated tools for the reconstruction of the cortical surface (Fischl and Dale 2000). For every subject, FreeSurfer segments the cerebral cortex, the white matter, and other subcortical structures and then computes meshes with ≈160 000 triangles that recover the geometry and the topology of the pial surface and the gray/white interface of the left and right hemispheres. The local cortical thickness is measured based on the distance between the position of homologous vertices in the pial and gray/white surfaces. A correspondence between the cortical surfaces across subjects is established using a nonlinear alignment of the principal sulci in each subject's brain with an average brain (Desikan et al. 2006). Brain volume was estimated using the BrainSegVol variable, a measure of the total brain volume (including ventricles and excluding intrasulcal spaces).

We extracted 2 different measures from each pial surface generated for each individual: total surface area and an overall folding ratio. Total surface area is simply the sum of the areas of each triangle in the final reconstructed pial surface. A measure of the overall folding was estimated as the ratio between the surface of the brain (S_b) and the surface area of a sphere of equal volume to the brain volume (S). The radius of such a sphere can be calculated explicitly (i.e., $V_b = (4/3)\pi r^3$, where r is radius of a sphere with the same volume as the brain [V_b]). By solving for r and substituting into the equation for a surface area of a sphere, we obtain the following expression for the folding ratio:

$$\ln\left(\frac{S_b}{S}\right) = \ln(S_b) - \frac{2}{3}\ln(V_b) - \frac{1}{3}\ln(36\pi).$$

Genetic Analyses

All adolescents ($n = 602$) were genotyped with the Illumina Human610-Quad BeadChip (Illumina, Inc., San Diego, CA) that includes 582 539 single nucleotide polymorphisms (SNPs) distributed across 22 autosomal chromosomes. The genotyping was conducted at the Centre National de Génotypage (Paris, France) where genotype calling was made for 567 726 SNPs. SNPs with call rate < 95% and minor allele frequency < 0.01 and SNPs that were not in Hardy–Weinberg equilibrium ($P < 1.0 \times 10^{-4}$) were excluded; a total of 530 011 SNPs

Table 1
Description of the discovery sample (Saguenay Youth Study)

	Girls		Boys	
	Nonexposed	Exposed	Nonexposed	Exposed
Alcohol during pregnancy (% mothers)	**20**	**30**	**16**	**34**
Wine during pregnancy (glasses/week)	0.4 (0.3)	0.6 (1.4)	0.2 (0.3)	0.5 (0.5)
Beer during pregnancy (bottles/week)	0.8 (0.9)	0.5 (0.4)	0.6 (0.7)	0.9 (0.8)
Second hand smoking during pregnancy at home (%mothers)	**21**	**56**	**25**	**64**
Second hand smoking during pregnancy at work (%mothers)	46	62	51	63
Pregnancy duration (weeks)	39.3 (1.5)	39.2 (1.4)	39.1 (1.5)	39.1 (1.6)
Maternal age at delivery (years)	27.3 (3.9)	26.7 (3.8)	27.2 (3.9)	26.7 (4.4)
Emergency C-section (%deliveries)	9	6	6	4
Elective C-section (%deliveries)	10	11	**17**	**8**
Birth weight (g)	**3481 (475)**	**3156 (481)**	**3601 (478)**	**3317 (444)**
Breastfeeding (% children)	**59**	**31**	**60**	**39**
Exclusive breastfeeding duration (weeks)	12.4 (9.9)	11.9 (10.7)	11.8 (8.6)	9.6 (7.1)
Postnatal depression (%mothers)	4	10	5	11
Maternal education during pregnancy (1 through 9)	**4.8 (1.4)**	**4.4 (1.2)**	4.3 (1.2)	4.4 (1.3)
Paternal education during pregnancy (1 through 9)	4.9 (1.7)	4.6 (1.6)	**4.9 (1.5)**	**4.4 (1.4)**
Maternal education at present (1 through 9)	4.9 (1.5)	4.7 (1.4)	4.5 (1.3)	4.8 (1.4)
Paternal education at present (1 through 9)	5.1 (1.7)	4.8 (1.6)	5.1 (1.6)	4.7 (1.5)
Household income at present (Canadian Dollars)	53 714 (24 680)	54 685 (26 559)	56 431 (23 174)	52 373 (26 105)

Note: Maternal/Paternal Education: 1 = primary not finished, 2 = primary finished, 3 = high school not finished, 4 = high school finished, 5 = high school not finished, 6 = high school finished, 7 = university not finished, 8 = bachelor degree, 9 = masters/PhD degree. Variables in bold indicate significant ($P < 0.05$) differences between exposed and nonexposed individuals in a given sex group. Unless otherwise indicated, means and SDs (in brackets) are reported.

passed these quality control criteria and were included in GWAS. On average, the call rate of these SNPs was 99.2%. In addition, 3 subjects were removed based on principal component analysis of population structure performed with HapMap3 (release 3) and SYS genotypes (Price et al. 2006), and one subject was excluded due to >3% of missing genotypes; the final number of adolescents was 598.

GWAS of brain volume was conducted with Merlin, version 1.1.2 (Abecasis et al. 2002, Abecasis and Wigginton 2005) under an additive model. With Merlin, a simple regression model is fitted to each trait, and a variance component approach is used to account for correlation between different observed phenotypes within each family. For individuals with missing genotypes, the Lander–Green algorithm is employed to estimate an expected genotype score (Lander and Green 1987). For brain volume, no values were outside mean ± 3 SDs. Age was included as a covariate. Quantile–quantile plot of GWAS-produced *P* values was prepared with WGAviewer, version 2 (Ge et al. 2008). Linkage disequilibrium (LD) structure of identified loci was examined in the SYS data set with HaploView 4.2 (Barrett et al. 2005). Nonadditivity was tested by including a heterozygote indicator in existing statistical models and testing its statistical significance. The heterozygote indicator was derived as follows: assuming $x = \{0, 1, 2\}$ is coded as number of minor alleles, then $X1 = (x - 1)$ and $X2 = 1$ if $x = 1$ or 0. Test for nonadditivity was H0: $\beta(X2) = 0$. Gene loci were considered statistically significant if their $P < 5 \times 10^{-8}$. These analyses were carried out separately in male ($n = 268$) and female ($n = 289$) adolescents.

As pointed out above, the discovery sample is drawn from a population with a known genetic founder effect. In founder populations, it is expected that fewer gene variants contribute to the determination of a complex trait, such as brain volume or cortical area studied here (Peltonen et al. 2000). The prevalence of several recessive disorders is higher in the Saguenay–Lac-Saint-Jean region than in other populations (De Braekeleer 1991), and limited allelic diversity exists among patients with these disorders (Grompe et al. 1994, De Braekeleer et al. 1998). It is expected that such a reduced genetic diversity, together with a wider LD intervals and a more homogenous (cultural) environment, facilitates the discovery of genetic variants associated with complex traits (Peltonen et al. 2000). On the other hand, it may also make results obtained in such populations less generalizable due to, for example, low frequency of certain genetic variants in the Saguenay population. Thus, we cannot exclude the possibility that our GWAS missed associations that would be detected in other samples. Note, however, that we did replicate the previous finding obtained with GWAS on total brain volume (*CDH4* locus, see below), which was carried out in mixed European ancestry (Seshadri et al. 2007).

Replication Sample: Avon Longitudinal Study of Parents and Children

We sought to replicate the observed interaction between *KCTD8* genotype and PEMCS vis-à-vis brain growth in an independent sample. Unfortunately, existing MR-based cohorts of typically developing children and adolescents (reviewed in Paus 2010b) do not include a sufficient number of "exposed" individuals. For this reason, we employ a large well-characterized birth cohort, namely the Avon longitudinal study of parents and children (ALSPAC), and used HC as a proxy of brain size. Brain weight is proportional to the cube of the HC from birth to 18 years of age (Epstein HT and Epstein EB 1978).

Participants

ALSPAC recruited >14 000 pregnant women resident in Avon, UK with expected dates of delivery from 1 April 1991 to 31 December 1992. Of these fetuses, 14 062 were live births and 13 988 were alive at 1 year. When the oldest children were approximately 7 years of age, an attempt was made to bolster the initial sample with eligible cases that failed to join the study originally. As a result, when considering variables collected from the age of 7 onward (and potentially abstracted from obstetric notes), there are data available for more than the 14 541 pregnancies mentioned above. Ethical approval for the study was obtained from the ALSPAC Law and Ethics Committee and the Local Research Ethics Committees. No specific exclusion or inclusion criteria have been used when selecting participants for this birth cohort.

HC of the Infant Shortly after Birth

A validation study of measurement of HC prior to the ALSPAC study had shown a high degree of inaccuracy in the measurements made in the maternity hospital. For the ALSPAC study, we therefore employed ALSPAC staff who had been trained in HC measurements by Maria Bredow. Dr Bredow had been trained by a team based at the Department of Professor Michael Preece of the Institute of Child Health, London. The team visited the 2 major maternity hospitals (Southmead and Bristol Maternity Hospital/St. Michael's) each morning and measured all available children for whom the mother gave permission (age of measurement post-birth is available).

HC at 7 Years of Age

HC was measured to the nearest millimeter at the widest horizontal circumference of the head as the child looked straight ahead. The tape was pulled tight to compress the hair.

Gestational Age

Gestation was calculated (in days) based on the date of the mother's last menstrual period, ultrasound assessments, or other clinical

indicators. Where maternal report and ultrasound assessment conflicted, an experienced obstetrician reviewed clinical records and made a best estimate. For the purposes of this analysis, gestation was rounded down to completed weeks.

Birth Weight

There were a variety of ways of identifying birth weight. This included the birth weight from obstetric data, birth weight as recorded by the ALSPAC measurers, and birth weight from birth notification. The preferred measure for birth weight was defined by using the following criteria—if all birth weights from each data set were identical, that was taken. If there was a difference between the recorded birth weights on the different data sets, then the criteria as described below were used: Omission where there are only 2 sources and they disagree by 100 g +. For those where the disagreement is <100 g, the lower figure has been taken.

Maternal Smoking

To ensure consistency with the inclusion criteria of the discovery sample (i.e., the Saguenay Youth Study), namely smoking one or more cigarettes per day during the second trimester (effectively smoking throughout pregnancy), we included infants born to mothers who reported "smoking regularly" on all 3 occasions when they were asked: during the first 3 months of their pregnancy, between 18 and 20 weeks of pregnancy, and during the last 2 months of pregnancy.

Information about smoking during the first 2 trimesters was derived from the "Having a Baby" questionnaires sent to the mother at 18–20 weeks' gestation. The specific aim of these questionnaires was to identify features of the mothers' lifestyle that might be important to fetal development. Information on the last 2 months of pregnancy (third trimester) was derived from the "Me and My Baby" questionnaire, which included a section on "Your Health & Lifestyle in Pregnancy."

Genetic Analyses

Genetic data. Genotyping was carried out at 2 different centres (The Wellcome Trust Sanger Centre, Cambridge, UK and Laboratory Corporation of America, Burlington, NC) using the Illumina Human550 quad array (Illumina, Inc.).

Quality control before imputation. Individuals were excluded on the basis of the following: sex mismatches, minimal or excessive heterozygosity, disproportionate levels of individual missingness (>3%), cryptic relatedness measured as proportion of identity by descent (IBD > 0.1), and insufficient sample replication (IBD < 0.8). The remaining individuals were assessed for evidence of population stratification by multidimensional scaling analysis and compared with Hapmap II (release 22) European descent (CEU), Han Chinese, Japanese, and Yoruba reference populations; all individuals with non-European ancestry were removed. Hidden population stratification was thereafter controlled for by using EIGENSTRAT (Price et al. 2006). SNPs with a minor allele frequency of <1%, a call rate of <95%, or evidence for violations of Hardy–Weinberg equilibrium ($P < 5 \times 10^{-7}$) were removed.

Imputation. Genotypic data were subsequently imputed using Markov Chain Haplotyping software (MACH v.1.0., Li et al. 2010), and phased haplotype data from CEU individuals (Hapmap release 22, Phase II NCBI B36, dbSNP 126) based on a cleaned data set of 8365 individuals and 464 311 autosomal SNPs. After imputation, all SNPs with indication of poor imputation quality (r^2 hat < 0.30) were removed.

Genotypic dosages used for main modeling are derived from genome-wide data. These are used in all but the interaction and means by genotype analysis where "best guess" genotypes were taken by rounding genetic dosages. As an indication of imputation quality, all genotypes from imputation had R^2 values exceeding 0.99. All analyses were undertaken assuming an additive genetic model. Gestational age and birth weight were used as covariates.

Meta-analysis of Expression Patterns

We assembled 19 publicly available expression-profiling studies of fetal mouse cells and tissue (680 microarrays). An aggregated coexpression network was generated by computing rank correlations among expression profiles in each experiment, converting absolute values of the correlations to ranks, and then summing ranks across the 19 experiments. We have shown that this method is a highly effective way of extracting functional information from expression data sets (Gillis and Pavlidis 2011). The coexpression score of each gene with *KCTD8* was extracted to produce a ranking. ErmineJ (Gillis et al. 2010) was used to compute enrichment of selected gene ontology categories in this ranking, using the "receiver-operator characteristic (ROC)" method. We also analyzed the human fetal brain expression data set of Johnson et al. 2009. We performed the same ROC analysis as for the mouse data; each gene and the gene ontology group identified as significant for *KCTD8* were reranked by how well they scored compared with their scores for all other genes. The details of the expression data and coexpression scores for *KCTD8* are available online at http://www.chibi.ubc.ca/Paus and in Supplementary Figure 1.

Results

Discovery Sample: The Saguenay Youth Study

In female adolescents, GWAS revealed an association between brain volume and several SNPs in the *KCTD8* locus located on chromosome 4 (Table 2 and Fig. 1); 6 SNPs with genome-wide significance ($P < 5.0 \times 10^{-08}$) were found (top SNP: rs716890, $P = 5.40 \times 10^{-09}$). The minor allele homozygotes and heterozygotes compared with the major allele homozygotes showed a smaller brain volume by 6.4% (Cohen's $d = 1.03$) and 5.2% ($d = 0.77$), respectively. The percent heritability explained by this SNP was 12.95%. In addition to this locus, nominal associations were

Table 2

KCTD8 locus in female adolescents (Saguenay Youth Study; $n = 290$) and age-adjusted brain volume (ccm, mean [standard error])

SNP	Allele 1	Allele 2	Frequency 1	MAF	*P* value	1-1	1-2	2-2
rs716890 (5)	G	T	0.24	0.24	5.4×10^{-09}	1178 (19)	1194 (8)	1256 (6)
rs7686284 (1)	A	G	0.29	0.29	8.2×10^{-09}	1188 (17)	1198 (7)	1260 (7)
rs1027201 (3)	C	T	0.71	0.29	8.2×10^{-09}	1260 (7)	1198 (7)	1188 (17)
rs6811002 (6)	C	T	0.27	0.27	9.3×10^{-09}	1185 (17)	1196 (8)	1256 (6)
rs7689563 (10)	A	G	0.25	0.25	1.1×10^{-08}	1178 (19)	1195 (8)	1256 (6)
rs17641380 (2)	C	T	0.26	0.26	1.8×10^{-08}	1181 (20)	1197 (7)	1257 (6)
rs7682929 (8)	A	C	0.20	0.20	2.1×10^{-08}	1180 (29)	191 (8)	1250 (6)
rs6447330 (11)	A	G	0.75	0.25	3.9×10^{-08}	1256 (6)	1196 (8)	1178 (19)
rs17599605 (9)	C	T	0.73	0.27	4.7×10^{-07}	1254 (7)	1201 (8)	1185 (18)
rs10007704 (7)	C	T	0.44	0.44	1.2×10^{-05}	1196 (12)	1222 (7)	1258 (9)
rs4695701 (4)	C	T	0.50	0.50	2.0×10^{-05}	1199 (10)	1223 (7)	1268 (10)

Note: 1-1, 1-2, and 2-2 indicate genotypes relative to allele 1 and allele 2. Note that Allele 1 is the minor allele in all but 3 cases (highlighted in gray). Carriers of a minor allele have smaller brain volume than major allele homozygotes. Numbers in brackets following the SNP identifiers correspond to those in Figure 1. MAF, minor allele frequency.

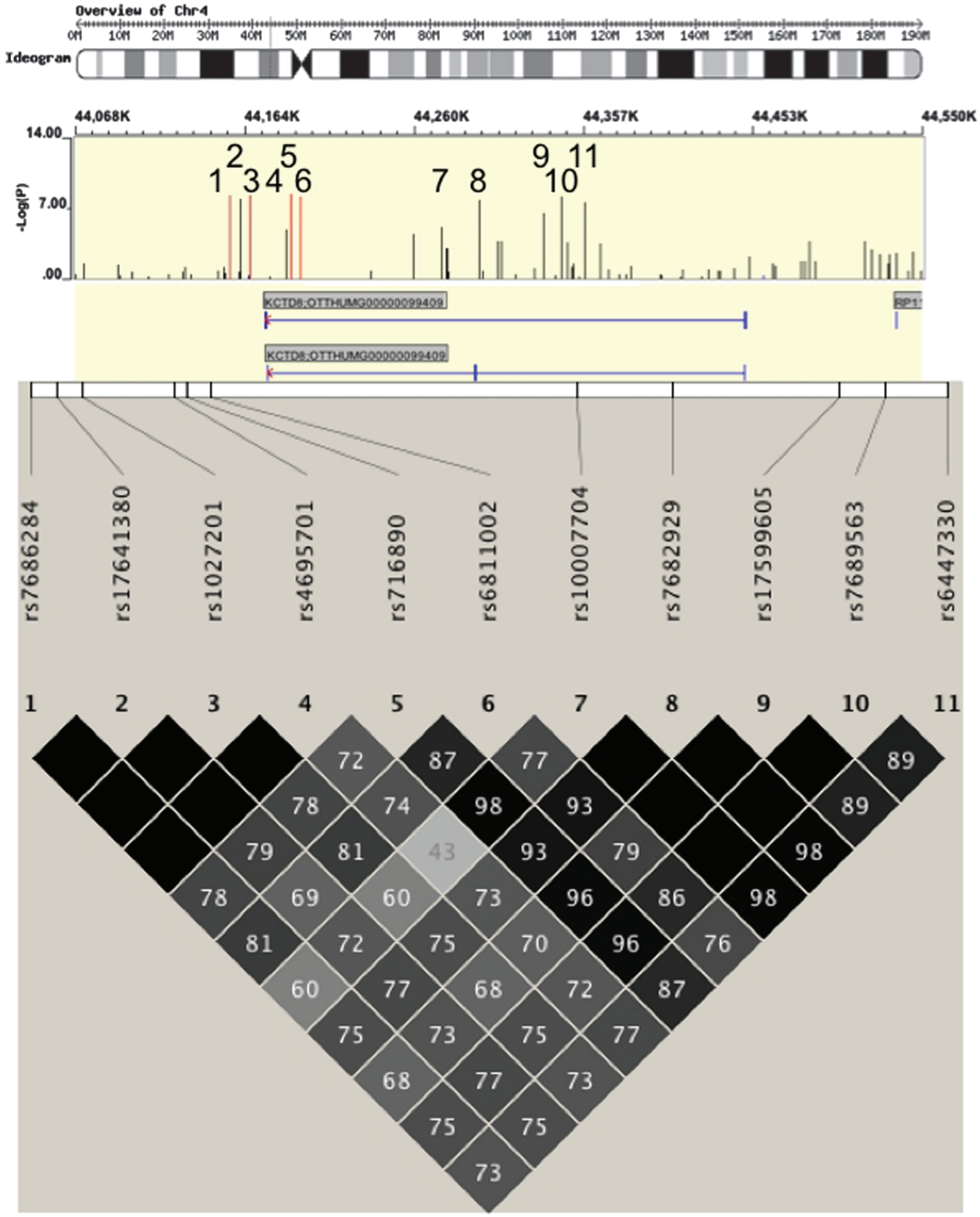

Figure 1. Top: results of the genome-wide analysis of brain volume in female adolescents, as shown by WGAviewer, version 2 (Ge et al. 2008). The top SNPs are indicated by numbers 1 through 11; SNPs 2,3, 5, and 6 (indicated in red) reached genome-wide significance ($P < 5.0 \times 10^{-08}$). Bottom: LD structure of the identified SNPs, as examined with HaploView 4.2 (Barrett et al. 2005) and indicated by D' values. Numbers identify the same SNPs shown in the top part of this figure.

detected at the *GATA4* (rs2409809, $P = 7.9 \times 10^{-06}$), *GRM7* (rs9864350, $P = 8.0 \times 10^{-06}$), and *FAM134B* (rs334493, $P = 9.8 \times 10^{-06}$) loci. In male adolescents, no genotype–phenotype associations were reliably detected ($P < 5.0 \times 10^{-08}$; Supplementary Table 1). Only 2 loci showed nominal association with brain volume: the *RPS14P7* (rs17040246, $P = 2.6 \times 10^{-06}$) and AC009518.5 (rs10271989, $P = 5.6 \times 10^{-06}$) loci. Finally, in both female and male adolescents, we replicated the previously reported (Seshadri et al. 2007) association between total brain volume and the *CDH4* locus (females: rs6061348, $P = 0.0001$; males: rs13045809, $P = 0.003$).

Next, we investigated the relationship between *KCTD8* and 3 global indicators of cortical development, namely the total cortical surface area, the overall degree of cortical folding (i.e., gyrification index), and mean cortical thickness (all adjusted for age). In female adolescents, we observed a relationship between *KCTD8* (rs716890) and the cortical surface area ($F_{2,290} = 14.7$, $P < 0.0001$ uncorrected for multiple comparisons, $P < 0.0001$ corrected for multiple comparisons) as well as cortical folding ($F_{2,290} = 4.2$, $P = 0.02$ uncorrected, $P = 0.06$ corrected) but not cortical thickness ($F_{2,290} = 0.3$, $P = 0.8$ uncorrected). No such effects were observed in male adolescents.

Given that the most sensitive period of cortical development takes place in utero, we decided to test the possibility of a modulating effect of PEMCS during pregnancy (exposure) on the above genotype–phenotype relationships. In female adolescents, there was evidence for an interaction between *KCTD8* (rs716890) and exposure for both the cortical surface area ($F_{2,290}$ = 6.4, P = 0.002 uncorrected, P = 0.01 corrected) and cortical folding ($F_{2,290}$ = 5.4, P = 0.005 uncorrected, P = 0.03 corrected) but not the cortical thickness ($F_{2,290}$ = 1.7, P = 0.2 uncorrected) or brain volume ($F_{2,290}$ = 1.4, P = 0.2 uncorrected); there was a marginal main effect of exposure on brain volume ($F_{2,290}$ = 2.9, P = 0.09 uncorrected). Figure 2 depicts the effects of *KCTD8* genotype on the brain volume (top), cortical surface area (middle), and folding (bottom) in the exposed and nonexposed female adolescents. Note that in the exposed females, the genotype explains 21.8% and 11.2% of the variation in cortical surface area and folding, respectively. In male adolescents, there was no evidence for the main effects of the *KCTD8* genotype or exposure not for genotype-by-exposure interactions on any of the brain and cortical phenotypes, with an exception of a genotype effect on cortical surface area ($F_{2,267}$ = 2.9, P = 0.05 uncorrected) driven by 3 minor-allele homozygotes.

We also evaluated possible main effects of the *KCTD8* genotype (rs716890) and its interaction with exposure on several measures of general growth, including birth weight,

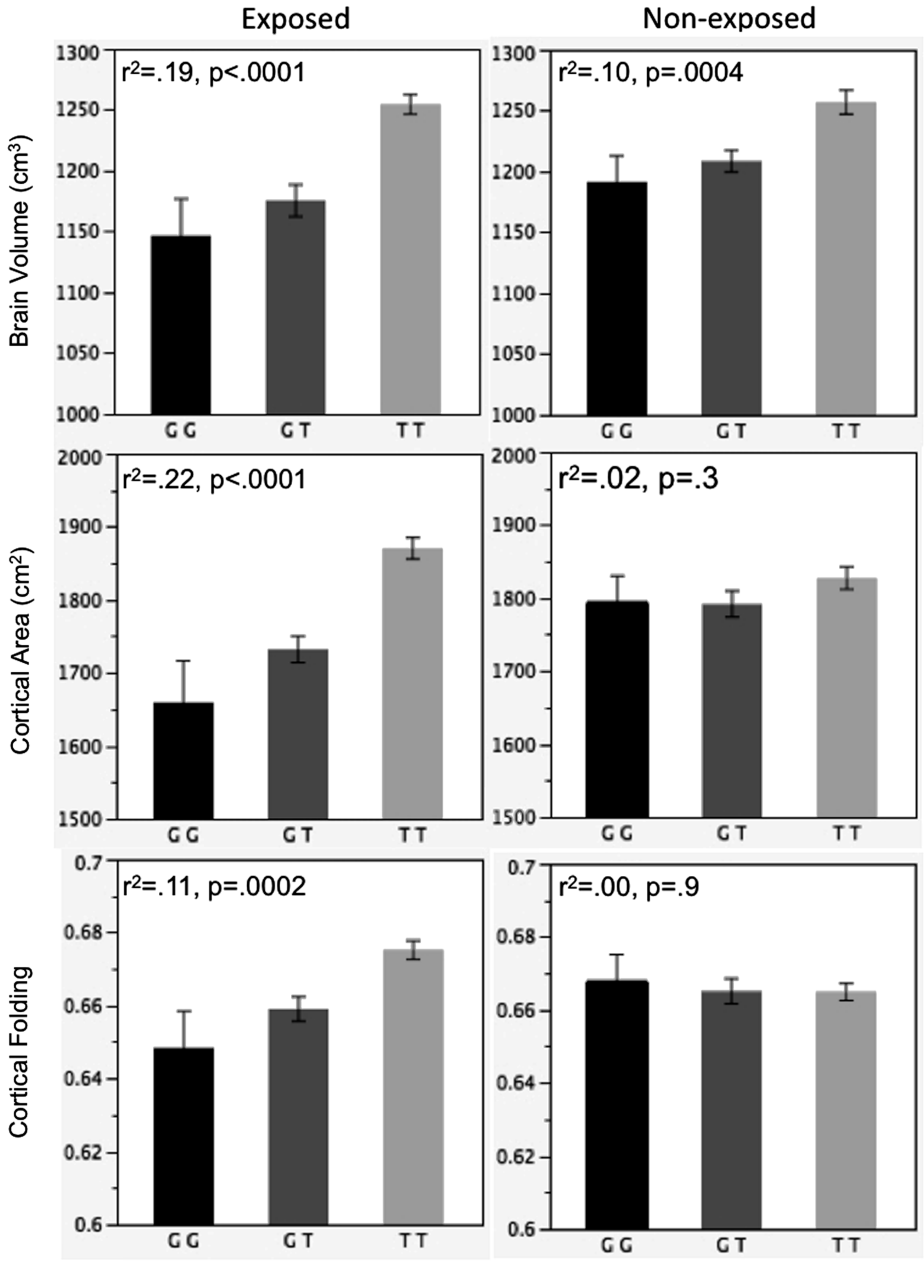

Figure 2. Age-adjusted values (mean ± standard error) of brain volume (top), total cortical area (middle), and cortical folding (bottom) in female adolescents exposed (left column) and not exposed (right column) to maternal cigarette smoking during pregnancy, all plotted as a function of the *KCTD8* genotype (rs716890; GG, GT, and TT genotypes; G, guanine; T, thymine). The amount of variance (r^2) explained by the genotype and statistical significance of the genotype effect of each phenotype are indicated. Note that we observed significant interaction between the *KCTD8* genotype (rs716890) and "exposure" on total cortical area and cortical folding but not on brain volume.

birth height, and current height (age adjusted), but there was no evidence of any effects in either the female or male adolescents (all $P > 0.1$ uncorrected).

Replication Sample: ALSPC

Using the top 11 SNPs in the *KCTD8* locus (Table 1), we tested the association between *KCTD8* genotypes and HC in the exposed female participants from the ALSPAC cohort. An association between *KCTD8* genotype and HC was considered a replication if there was nominal evidence against the null hypothesis ($P < 0.05$) and the direction of effect was consistent. In the case of HC measured at birth (532 exposed females), there was no replication of the original findings (Supplementary Table 2A). In the case of HC measured at 7 years of age (437 exposed females), 2 of 11 SNPS replicated the original findings (Supplementary Table 2B). An interaction between *KCTD8* genotype and PEMCS vis-à-vis HC at 7 years of age was found for 2 of 11 SNPs (Supplementary Table 2B); this analysis included 437 exposed females and 2164 nonexposed females. Finally, we have tested an association between *KCTD8* and head growth, defined as a difference in HC between 7 years of age and birth (335 exposed females); this association was found for 1 of 11 SNPs (rs17599605, $P = 0.007$) and indicated a lower growth in minor allele carriers. The same SNP showed an interaction with exposure, with a lower HC growth observed in the exposed females ($P = 0.04$). Note that measurements of HC shortly after birth may be a less reliable proxy of brain size due to the head deformation occurring during vaginal delivery, especially in primiparas (Sorbe and Dahlgren 1983). No evidence of the effects of *KCTD8* genotype and/or interaction with PEMCS was found in male participants from the ALSPAC cohort.

Meta-analysis of Expression Patterns

The function of *KCTD8* is not well described, being associated with gene ontology terms only by virtue of its inferred protein sequence (e.g., potassium ion transport). To gain further insight into *KCTD8* function, we used a meta-analysis approach to analyze expression networks of *KCTD8* across 680 microarrays from fetal mouse cells and tissue. We scored these networks for enrichment in functions of interest. The results confirm the functions inferred from its protein sequence. Genes coexpressed with *KCTD8* in fetal mouse (corrected $P < 0.01$, genes listed have ranks > 99.5%) are enriched for genes playing roles in potassium ion transport (*KCNC3*), development (e.g., *NRG3*, *NRCAM*), and neurotransmission (e.g., *Slc6a13*, *Slc7a10*, Slc6a3); see Supplementary Figure 1 for the full coexpression network. In addition to the fetal mouse tissue, we examined a gene expression network constructed from a much smaller set of data on human fetal brain (Johnson et al. 2009). In this data set, we might expect many genes to be enriched for brain functions, so we corrected for this possible bias by performing coexpression enrichment analysis for each gene on the array and determining the gene ontology groups for which *KCTD8* was particularly enriched. Consistent with the findings from the mouse data, *KCTD8*'s coexpression partners were particularly linked to brain-related ontologies, such as "neuron fate commitment," "neural crest cell migration," and "neurotransmitter metabolic process." These represent 3 of the top 5 gene ontology groups in which *KCTD8* was more enriched than all but 0.6% of other genes, thus correcting for the fact that the (fetal brain) data set might be biased in favor of such findings.

Discussion

We found an association between the polymorphism of *KCTD8* and brain volume. Furthermore, *KCTD8* seems to modulate the adverse effects of PEMCS on cortical surface area and cortical folding, as determined with MRI in typically developing female adolescents recruited in a population with a known genetic founder effect. *KCTD8* belongs to a family of genes (21 members) that share a conserved sequence characteristic for the tetramerization domain of voltage-gated potassium channels. The tetramerization domain (T1) is a part of the intracellular amino-terminal polypeptide chain that controls the specificity of tetramerization of voltage-gated potassium channels; it is also possible that T1 affects permeation of K+ through the channel pore (Sansom 1998, Yi et al. 2001). Certain mutations in T1 result in nonfunctional potassium channels, possibly through conformational changes affecting the state (closed/open) of the channel (Minor et al. 2000, Yi et al. 2001). Some of the members of the *KCTD* family, such as *KCTD12*, are highly expressed in the developing brain (http://developingmouse.brain-map.org), others (*KCTD1*, *KCTD10*) are known to interact with transcription factors (activator protein 2 [*AP-2*]) involved in neurodevelopment (Ding et al. 2009, Liu et al. 2009).

Apoptosis is one of the key regulators of the final number of cells constituting the cerebral cortex, affecting both the number of progenitor cells and (surviving) the postmitotic neurons. A higher rate of apoptosis has been observed in the neuroepithelium of whole-rat embryo cultures exposed to nicotine, as compared with control embryos (Roy et al. 1998). Prenatal exposure to nicotine appears to downregulate anti-apoptotic pathways, thus increasing vulnerability to hypoxia-induced apoptosis (Simakajornboon et al. 2010). A reduction of intracellular levels of potassium ($[K^+]_i$) may be one of the permissive signals in apoptosis (Yu 2003). It has been shown that low $[K^+]_i$ decreases DNA-binding activity of antiapoptotic (cAMP response element-binding) transcription factors and increases binding activity of proapoptotic (p53 and Forkhead) transcription factors (Yang et al. 2006). We speculate that genetic variation in *KCTD8* might modulate hypoxia-induced loss of intracellular potassium and, in turn, promote apoptosis in the developing brain. During the first trimester, such an effect would lead to a reduction in the number of progenitor cells, with exponential consequences on the final number of neurons (Rakic 1995) and the total area of the cortical sheath. During the second and third trimester, such a mechanism would lead to a reduction of postmitotic neurons in the cerebral cortex. After birth, the latter effects might continue owing to the second-hand exposure of the infant to cigarette smoke.

It should be noted that the modulating effect of cigarette smoking during pregnancy on the association between *KCTD8* and the cortical area/folding cannot be attributed solely to the effect of chemicals contained in cigarette smoke or to the prenatal period. Mothers who smoked during pregnancy also reported more frequent use of alcohol, albeit in moderate amounts. After birth, mothers of exposed children continued to smoke and were less likely to breastfeed their offspring. Thus, exposure to maternal cigarette smoking during pregnancy should be viewed only as a proxy of an adverse prenatal and early

postnatal environment rather than a sole causative factor. Experimental studies carried out in in vivo and in vitro are needed to identify the key factors, sensitive periods, and mediating mechanisms as well as to establish causality in the relationship between *KCTD8*, exposure, and cortical development.

The interaction between *KCTD8* genotype and exposure was observed only in female offspring. This was the case for both the brain phenotypes (The Saguenay Youth Study) and the HC (ALSPAC). Using MRI data collected in the Saguenay Youth Study, we have reported previously on the association between maternal cigarette smoking during pregnancy and the (absolute and relative) size of the corpus callosum (Paus et al. 2008); the effect of exposure was present only in female adolescents. Given that no differences between exposed and nonexposed adolescents were found in the myelination index, we concluded that the observed size difference might reflect that in the number of axons. What could protect male adolescents from the adverse effects of PEMCS on the developing brain? Is it possible that androgens, produced in utero by the testes of the male fetus, offer such a protection? It is known, for example, that androgens protect against apoptosis in hippocampal neurons (Nguyen et al. 2010). Testosterone may affect apoptosis by modulating directly expression of pro- and antiapoptotic genes or regulate availability of neurotrophic factors (Forger 2009). Testosterone levels in the amniotic fluid of male fetuses are high as early as in week 15 of gestation, the earliest time such measurements are available (Sarkar et al. 2007). Thus, the lack of an interaction between *KCTD8* genotype and exposure on the area and folding of the cerebral cortex in male adolescents might be related to such a protective effect of androgens in utero.

Supplementary Material

Supplementary material can be found at: http://www.cercor.oxfordjournals.org/

Funding

The Saguenay Youth Study project is funded by the Canadian Institutes of Health Research (T.P. [NET 54015, MOP 86678], Z.P. [MOP-74623, MOP-79571]) and the Canadian Foundation for Innovation (Z.P.; Project CFI# 6862). UK Medical Research Council (grant ref: 74882), Wellcome Trust (grant ref: 076467), and University of Bristol provide core support for ALSPAC.

Notes

We thank all families who took part in the Saguenay Youth Study and the following individuals for their contributions in designing the protocol, acquiring, and analyzing the data: psychometricians (Chantale Belleau, Mélanie Drolet, Catherine Harvey, Stéphane Jean, Hélène Simard, Mélanie Tremblay, and Patrick Vachon), ÉCOBES team (Nadine Arbour, Julie Auclair, Marie-Ève Blackburn, Marie-Ève Bouchard, Annie Houde, and Catherine Lavoie), laboratory technicians (Denise Morin and Nadia Mior), Julie Bérubé, Celine Bourdon, Rosanne Aleong, Dr Jennifer Barrett, Candice Cartier, Dale Einarson, Helena Jelicic, and Valerie Legge. We thank Dr Jean Mathieu for the medical follow-up of participants in whom we detected any medically relevant abnormalities. We thank Manon Bernard for designing and managing our online database. We are extremely grateful to all ALSPAC families who took part in this study, the midwives for their help in recruiting them, and the whole ALSPAC team, which includes interviewers, computer and laboratory technicians, clerical workers, research scientists, volunteers, managers, receptionists, and nurses. We also acknowledge funding by the EC-FP-6 Integrated Project "IMAGEN" (LSHM-CT-2007-037286). This publication is the work of the authors and Drs Nicholas Timpson and George Davey Smith will serve as ALSPAC guarantors for the contents of this paper. *Conflict of Interest*: None declared.

References

Abecasis GR, Cherny SS, Cookson WO, Cardon LR. 2002. Merlin-rapid analysis of dense genetic maps using sparse gene flow trees. Nat Genet. 30:97–101.

Abecasis GR, Wigginton JE. 2005. Handling marker-marker linkage disequilibrium: pedigree analysis with clustered markers. Am J Hum Genet. 77:754–767.

Barrett JC, Fry B, Maller J, Daly MJ. 2005. Haploview: analysis and visualization of LD and haplotype maps. Bioinformatics. 21:263–265.

Chan WY, Lorke DE, Tiu SC, Yew DT. 2002. Proliferation and apoptosis in the developing human neocortex. Anat Rec. 267:261–276.

Chan WY, Yew DT. 1998. Apoptosis and Bcl-2 oncoprotein expression in the human fetal central nervous system. Anat Rec. 252:165–175.

De Braekeleer M. 1991. Hereditary disorders in Saguenay-Lac-St-Jean (Quebec, Canada). Hum Hered. 41:141–146.

De Braekeleer M, Mari C, Verlingue C, Allard C, Leblanc JP, Simard F, Aubin G, Férec C. 1998. Complete identification of cystic fibrosis transmembrane conductance regulator mutations in the CF population of Saguenay Lac-Saint-Jean (Quebec, Canada). Clin Genet. 53:44–46.

Desikan RS, Ségonne F, Fischl B, Quinn BT, Dickerson BC, Blacker D, Buckner RL, Dale AM, Maguire RP, Hyman BT, et al. 2006. An automated labeling system for subdividing the human cerebral cortex on MRI scans into gyral based regions of interest. Neuroimage. 31:968–980.

Ding X, Luo C, Zhou J, Zhong Y, Hu X, Zhou F, Ren K, Gan L, He A, Zhu J, et al. 2009. The interaction of KCTD1 with transcription factor AP-2alpha inhibits its transactivation. J Cell Biochem. 106:285–295.

Epstein HT, Epstein EB. 1978. The relationship between brain weight and head circumference from birth to age 18 years. Am J Phys Anthropol. 48:471–473.

Fischl B, Dale AM. 2000. Measuring the thickness of the human cerebral cortex from magnetic resonance images. Proc Natl Acad Sci USA. 97:11050–11055.

Forger NG. 2009. Control of cell number in the sexually dimorphic brain and spinal cord. J Neuroendocrinol. 21:393–399.

Ge D, Zhang K, Need AC, Martin O, Fellay J, Urban TJ, Telenti A, Goldstein DB. 2008. WGAViewer: software for genomic annotation of whole genome association studies. Genome Res. 18:640–643.

Giedd JN, Schmitt JE, Neale MC. 2007. Structural brain magnetic resonance imaging of pediatric twins. Hum Brain Mapp. 28:474–481.

Gillis J, Mistry M, Pavlidis P. 2010. Gene function analysis in complex data sets using ErmineJ. Nat Protoc. 5:1148–1159.

Gillis J, Pavlidis P. 2011. The role of indirect connections in gene networks in predicting function. Bioinformatics. 27:1860–1966.

Grompe M, St-Louis M, Demers SI, al-Dhalimy M, Leclerc B, Tanguay RM. 1994. A single mutation of the fumarylacetoacetate hydrolase gene in French Canadians with hereditary tyrosinemia type I. N Engl J Med. 331:353–357.

Guerrini I, Thomson AD, Gurling HD. 2007. The importance of alcohol misuse, malnutrition and genetic susceptibility on brain growth and plasticity. Neurosci Biobehav Rev. 31:212–220.

Johnson MB, Kawasawa YI, Mason CE, Krsnik Z, Coppola G, Bogdanović D, Geschwind DH, Mane SM, State MW, Sestan N. 2009. Functional and evolutionary insights into human brain development through global transcriptome analysis. Neuron. 62:494–509.

Knickmeyer RC, Gouttard S, Kang C, Evans D, Wilber K, Smith JK, Hamer RM, Lin W, Gerig G, Gilmore JH. 2008. A structural MRI study of human brain development from birth to 2 years. J Neurosci. 28:12176–12182.

Kuan CY, Roth KA, Flavell RA, Rakic P. 2000. Mechanisms of programmed cell death in the developing brain. Trends Neurosci. 23:291–297.

Lambers DS, Clark KE. 1996. The maternal and fetal physiologic effects of nicotine. Semin Perinatol. 20:115–126.

Lander ES, Green P. 1987. Construction of multilocus genetic linkage maps in humans. Proc Natl Acad Sci U S A. 84:2363–2367.

Li Y, Willer CJ, Ding J, Scheet P, Abecasis GR. 2010. MaCH: using sequence and genotype data to estimate haplotypes and unobserved genotypes. Genet Epidemiol. 34:816–834.
Liu R, Zhou A, Ren D, He A, Hu X, Zhang W, Yang L, Liu M, Li H, Zhou J, et al. 2009. Transcription factor specificity protein 1 (SP1) and activating protein 2alpha (AP-2alpha) regulate expression of human KCTD10 gene by binding to proximal region of promoter. FEBS J. 276:1114–1124.
Minor DL, Lin YF, Mobley BC, Avelar A, Jan YN, Jan LY, Berger JM. 2000. The polar T1 interface is linked to conformational changes that open the voltage-gated potassium channel. Cell. 102:657–670.
Mochida GH. 2009. Genetics and biology of microcephaly and lissencephaly. Semin Pediatr Neurol. 16:120–126.
Nguyen TV, Jayaraman A, Quaglino A, Pike CJ. 2010. Androgens selectively protect against apoptosis in hippocampal neurones. J Neuroendocrinol. 22:1013–1022.
Opitz JM, Holt MC. 1990. Microcephaly: general considerations and aids to nosology. J Craniofac Genet Dev Biol. 10:175–204.
Paus T. 2010a. Sex differences in the human brain: a developmental perspective. Prog Brain Res. 186:13–28.
Paus T. 2010b. Population Neuroscience: why and how. Hum Brain Mapp. 31:891–903.
Paus T, Nawazkhan I, Leonard G, Perron M, Pike GB, Pitiot A, Richer L, Veillette S, Pausova Z. 2008. Corpus callosum in adolescent offspring exposed prenatally to maternal cigarette smoking. Neuroimage. 40:435–441.
Pausova Z, Paus T, Abrahamowicz M, Almerigi J, Arbour N, Bernard M, Gaudet D, Hanzalek P, Hamet P, Evans AC, et al. 2007. Genes, maternal smoking, and the offspring brain and body during adolescence: design of the Saguenay Youth Study. Hum Brain Mapp. 28:502–518.
Peltonen L, Palotie A, Lange K. 2000. Use of population isolates for mapping complex traits. Nat Rev Genet. 1(3):182–190.
Price AL, Patterson NJ, Plenge RM, Weinblatt ME, Shadick NA, Reich D. 2006. Principal components analysis corrects for stratification in genome-wide association studies. Nat Genet. 38:904–909.
Rakic P. 1995. A small step for the cell, a giant leap for mankind: a hypothesis of neocortical expansion during evolution. Trends Neurosci. 18:383–388.
Rakic S, Zecevic N. 2000. Programmed cell death in the developing human telencephalon. Eur J Neurosci. 12:2721–2734.
Roy TS, Andrews JE, Seidler FJ, Slotkin TA. 1998. Nicotine evokes cell death in embryonic rat brain during neurulation. J Pharmacol Exp Ther. 287:1136–1144.
Sansom MS. 1998. Ion channels: a first view of K+ channels in atomic glory. Curr Biol. 8:R450–R452.
Sarkar P, Bergman K, Fisk NM, O'Connor TG, Glover V. 2007. Amniotic fluid testosterone: relationship with cortisol and gestational age. Clin Endocrinol (Oxford). 67:743–747.
Seshadri S, DeStefano AL, Au R, Massaro JM, Beiser AS, Kelly-Hayes M, Kase CS, D'Agostino RB Sr, Decarli C, Atwood LD, et al. 2007. Genetic correlates of brain aging on MRI and cognitive test measures: a genome-wide association and linkage analysis in the Framingham Study. BMC Med Genet. 19(Suppl 1):S15.
Simakajornboon N, Kuptanon T, Jirapongsuwan P. 2010. The effect of prenatal nicotine exposure on PDGFR-mediated anti-apoptotic mechanism in the caudal brainstem of developing rat. Neurosci Lett. 478:46–50.
Slotkin TA. 1998. Fetal nicotine or cocaine exposure: which one is worse? J Pharmacol Exp Ther. 85:931–945.
Sorbe B, Dahlgren S. 1983. Some important factors in the molding of the fetal head during vaginal delivery—a photographic study. Int J Gynaecol Obstet. 21:205–212.
Toro R, Leonard G, Lerner JV, Lerner RM, Perron M, Pike GB, Richer L, Veillette S, Pausova Z, Paus T. 2008. Prenatal exposure to maternal cigarette smoking and the adolescent cerebral cortex. Neuropsychopharmacology. 33:1019–1027.
Yang Q, Yan D, Wang Y. 2006. K+ regulates DNA binding of transcription factors to control gene expression related to neuronal apoptosis. Neuroreport. 17:1199–1204.
Yi BA, Minor DL Jr, Lin YF, Jan YN, Jan LY. 2001. Controlling potassium channel activities: interplay between the membrane and intracellular factors. Proc Natl Acad Sci U S A. 98:11016–11023.
Yu SP. 2003. Regulation and critical role of potassium homeostasis in apoptosis. Prog Neurobiol. 70:363–386.